694 *Macromolecules* **2011**, *44*, 694–702
DOI: 10.1021/ma102717d

Macromolecules
ARTICLE

Poly(arylene ether sulfone) Statistical Copolymers Bearing Perfluoroalkylsulfonic Acid Moieties

Haibo Li, Andrew B. Jackson, Nathan J. Kirk, Kenneth A. Mauritz, and Robson F. Storey*

School of Polymers and High Performance Materials, The University of Southern Mississippi, Hattiesburg, Mississippi 39406, United States

Received April 12, 2010; Revised Manuscript Received January 6, 2011

ABSTRACT: The perfluoroalkylsulfonate monomer, *N,N*-diisopropylethylammonium 2,2-bis(*p*-hydroxyphenyl)pentafluoropropanesulfonate (HPPS), was synthesized in three steps. Using triethyl phosphite, hexafluoroacetone was first converted to ethyl pentafluoroisopropenyl ether. Reaction of the ether with sulfur trioxide produced 2-ketopentafluoropropanesulfonic acid. The acid was condensed with 2 equiv of phenol, and the product was isolated as the *N,N*-diisopropylethylammonium salt. The structure of the final product was confirmed by X-ray crystallography. Poly(arylene ether sulfone)s (PAES) were prepared by homopolymerization of HPPS with bis(4-fluorophenyl) sulfone (FPS) and copolymerization of varying molar ratios of HPPS/biphenol (BP) with FPS. Copolymer number-average molecular weights were in the range 27 000−34 000 g/mol (GPC). Copolymer compositions ranged from 20 to 61 mol % HPPS (HPPS/BP molar ratio 0.25−1.56) as determined by ^{19}F NMR spectroscopy. Ion exchange capacity of the copolymers (by titration) ranged from 0.36 to 1.25 mequiv/g. Equilibrium water uptake of the copolymers at 80 °C and 90% relative humidity increased from 7.2 to 14.3 mol H_2O/mol H^+, and proton conductivity increased from 1.6 to 23 mS/cm, as the HPPS/PB ratio increased from 0.25 to 1.56.

Introduction

A fuel cell produces electricity cleanly by an electrochemical process rather than through combustion. Since this avoids the intermediate steps of heat generation and conversion to mechanical work typical of most conventional power generation methods, the thermodynamic efficiency limitations of a heat engine (Carnot cycle) are avoided. A single fuel cell contains a cathode and an anode, separated by a solid polyelectrolyte, i.e., a polymeric proton exchange membrane (PEM).[1] In addition to physically separating the cathode and anode, the membrane must serve as a barrier to diffusion of hydrogen and oxygen, and it must facilitate passage of hydrogen cations across the cell with very low resistance.[1]

For ~40 years, benchmark fuel cell membrane materials have consisted of polymers with a perfluorinated polyethylene main chain and perfluoroether side chains terminated with sulfonic acid groups, for example, Nafion. Because of the amphiphilic nature of this polymer and its strongly acidic $-CF_2SO_3H$ groups, phase separation occurs to create hydrophilic proton conducting channels within a hydrophobic matrix. Its perfluorinated structure gives rise to high chemical and oxidative stability. Nafion and similar materials do have disadvantages, however. They are relatively expensive, primarily as a result of their high fluorine content. They exhibit low conductivity under low humidity conditions, display relatively low mechanical strength at higher temperatures, and possess moderate glass transition temperatures.[2] These disadvantages have provided an impetus for development of new, alternative membrane materials.[3−5]

A number of different approaches have been taken toward development of new fuel cell membrane materials including direct polymer/inorganic composites,[4,6,7] polymerization of organic polymers from inorganic initiators,[8,9] and creation, by step-growth polymerization, of high-performance aromatic polymers.[10−12] Prominent among the latter are sulfonated poly(arylene ether sulfone)s (sPAES) and sulfonated polyimides. These polymer families possess rigid, aromatic backbones that confer membrane mechanical stability and high thermal and oxidative resistance by virtue of the absence of aliphatic C−H bonds. Since the sulfonic acid groups of these ion-exchange polymers are typically bonded directly to the phenyl rings of the backbone, they are expected to be less strongly acidic than the $-CF_2SO_3H$ groups of Nafion and other perfluorosulfonic acid polymers; this can potentially influence performance properties such as water uptake and proton conductivity at a given ion exchange capacity (IEC).

Much of the pioneering work on sPAES polymers has been carried out by McGrath and co-workers.[11,13−17] They have shown that sPAES possess many desirable properties such as easy preparation, easy functionalization, thermo- and chemical stability, relatively low cost, and excellent mechanical performance.

In this report, we describe the preparation of new poly(arylene ether sulfone) (PAES) membrane polymers combining some desirable features of both sPAES and perfluorosulfonic acid polymers such as Nafion. As shown in Scheme 1, these polymers are similar to sPAES except that the sulfonic acid groups, rather than being connected directly to the aromatic rings of the backbone, are attached via a perfluoroalkyl group. The key element of these polymers is the ion-containing bisphenolic monomer, *N,N*-diisopropylethylammonium 2,2-bis(*p*-hydroxyphenyl)pentafluoropropanesulfonate (HPPS).

Experimental Section

Materials. Hexafluoroacetone was purchased from SynQuest Laboratories, Inc. (Alachua, FL) and used as received. Triethyl phosphite was purchased from Sigma-Aldrich and distilled from a flask containing sodium, to remove water and any dialkyl phosphonate; the distillate was collected over dried molecular

---

*Corresponding author. E-mail: Robson.Storey@usm.edu.

Scheme 1. Preparation of Poly(arylene ether sulfone) (PAES) Made from HPPS, BF, and FPS

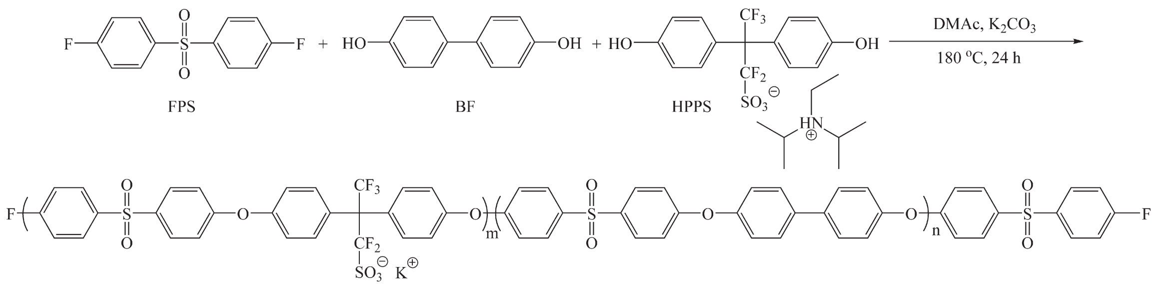

sieves. Phenol (99%), trifluoroacetic acid (99%), *N,N*-diisopropylethylamine (99%), LiBr (99%), DMAc (99.8%), DMF (HPLC grade), sulfur trioxide (99%), chloroform-*d* (99.8%), methanol-*d* (99.8%), and DMSO-d_6 (99.9%) were used as received from Sigma-Aldrich. Prior to use, sulfur trioxide was stored at 37 °C to avoid polymerization. K_2CO_3 (99.7%) was used as received from Fisher Scientific. Bis(4-fluorophenyl) sulfone (FPS) (99.0%, Sigma-Aldrich) was purified by recrystallization from toluene, and biphenol (BP) (97.0%, Sigma-Aldrich) was purified by vacuum sublimation prior to polymerization.

Instrumentation. *Spectroscopy*. NMR spectra were acquired using Varian Mercury^{plus} 300 and 200 MHz NMR spectrometers. Samples were dissolved in chloroform-*d*, methanol-*d*, or DMSO-d_6 (3−7%, w/v) and analyzed using 5 mm NMR tubes. ATR-FTIR spectra were recorded on a Thermo Scientific Nicolet 6700 spectrometer equipped with a diamond crystal Smart Orbit ATR accessory.

Thermal Analysis. Thermal gravimetric analysis (TGA) was performed on a TA Instruments TGA Q50 using a temperature gradient of 10 °C/min; samples were ramped from 30 to 800 °C in a platinum pan under a nitrogen atmosphere. Differential scanning calorimetry (DSC) was performed using a TA Instruments DSC Q200 with a 10 °C/min heating rate under nitrogen.

Gel Permeation Chromatography. Number-average molecular weight (M_n) and polydispersity index (PDI) of the polymeric materials were measured using a gel permeation chromatography (GPC) system consisting of a Waters Alliance 2695 separation module, an online multiangle laser light scattering (MALLS) detector fitted with a gallium arsenide laser (power: 20 mW) operating at 690 nm (MiniDAWN, Wyatt Technology Inc.), an interferometric refractometer (Optilab DSP, Wyatt Technology Inc.), and two Polymer Laboratories mixed D columns (5 μm bead size) connected in series. HPLC grade DMF containing 0.02 M LiBr served as the mobile phase and was delivered at a flow rate of 0.5 mL/min. Sample concentrations were ca. 20 mg of polymer/mL of DMF, and the injection volume was 100 μL. The detector signals were simultaneously recorded using ASTRA software (Wyatt Technology Inc.), and absolute molecular weights were determined by MALLS using a d*n*/d*c* calculated from the response of the interferometric refractometer and assuming 100% mass recovery from the columns.

X-ray Crystallography. A pale brown, irregular specimen of $C_{23}H_{30}F_5NO_5S$, approximate dimensions 0.34 mm × 0.57 mm × 0.82 mm, was used for the X-ray crystallographic analysis. After coating with Paratone-N (Hampton Research) the sample was transferred immediately to the cold stream (100 K) of the diffractometer. The X-ray intensity data were measured using a Bruker APEX-2 diffractometer and Mo Kα (λ = 0.710 73 Å) radiation. A total of 1851 frames were collected. The total exposure time was 1.54 h. The frames were integrated with the Bruker SAINT software package using a narrow-frame algorithm. Integration of the data using a monoclinic unit cell yielded a total of 27 831 reflections to a maximum θ angle of 29.22° (0.73 Å resolution), of which 6427 were independent (average redundancy 4.330, completeness = 99.4%, R_{int} = 2.05%, R_{sig} = 1.64%) and 5883 (91.54%) were greater than $2\sigma(F2)$. The final cell constants, a = 10.9827(5) Å, b = 19.8498(9) Å, c = 10.9827(5) Å, and volume = 2388.0(2) Å^3, were based upon the refinement of the *XYZ*-centroids of 9960 reflections above $20\sigma(I)$ with $5.069° < 2\theta < 58.36°$. Data were corrected for absorption effects using the multiscan method (SADABS). The ratio of minimum to maximum apparent transmission was 0.905. The calculated minimum and maximum transmission coefficients (based on crystal size) were 0.8469 and 0.9325. The structure was solved and refined using the Bruker SHELXTL Software Package, using the space group P_{21}/n, with Z = 4 for the formula unit, $C_{23}H_{30}F_5NO_5S$. The final anisotropic full-matrix least-squares refinement on $F2$ with 325 variables converged at $R1$ = 3.26% for the observed data and $wR2$ = 9.20% for all data. The goodness-of-fit was 1.063. The largest peak in the final difference electron density synthesis was 0.506 e$^-$/Å^3, and the largest hole was −0.341 e$^-$/Å^3 with an rms deviation of 0.052 e$^-$/Å^3. On the basis of the final model, the calculated density was 1.467 g/cm^3. Elemental analysis was performed by Galbraith Laboratories, Knoxville, TN.

Synthesis of *N,N*-Diisopropylethylammonium 2,2-Bis(*p*-hydroxyphenyl)pentafluoropropanesulfonate (HPPS or 4) (Scheme 2). *Ethyl Pentafluoroisopropenyl Ether* (*1*). In an inert-atmosphere drybox, hexafluoroacetone (188 mL) was condensed into a graduated receiving vial at −60 °C and then transferred into a chilled reaction flask equipped with a mechanical stirrer. Distilled triethyl phosphite (295 g, 1.77 mol) was precooled (−60 °C) prior to dropwise addition (over the course of 90 min) to the neat hexafluoroacetone at −60 °C. A cloudy vapor formed immediately and remained in the flask throughout the addition. After addition the reaction was brought to room temperature and stirred for 2 h. A clear, light-yellow-green solution developed. Distillation of the mixture resulted in isolation of a clear, colorless liquid, ethyl pentafluoroisopropenyl ether (**1**) (247 g, bp = 50 °C; yield ≈79%, based on 25 °C density of hexafluoroacetone of 1.32 g/mol reported by vendor). **1** was stored in a sealed round-bottom flask at 0 °C and redistilled prior to sulfonation with SO_3. ^{1}H NMR ($CDCl_3$, 298 K, δ): 3.93 (q, 2H, CH_2), 1.30 (t, 3H, CH_3). ^{13}C NMR ($CDCl_3$, 298 K, δ): 14.5 (CH_3), 70.9 (CH_2), 112 (m, C=CF$_2$), 120.9 (ddq, CF_3, $^3J_{C-F(cis)}$ = 3 Hz, $^3J_{C-F(trans)}$ = 7 Hz, $^1J_{C-F}$ = 273 Hz), 156.6 (m, C=CF$_2$, $^3J_{C-F}$ = 4 Hz, $^1J_{C-F}$ = 297 Hz). ^{19}F NMR ($CDCl_3$, 298 K, δ): −67.4 (dd, 3F, CF_3, $^4J_{F-F(cis)}$ = 10 Hz, $^4J_{F-F(trans)}$ = 24 Hz), −90.8 (dq, 1F, C=CF_{cis} $^4J_{F-F}$ = 10 Hz, $^2J_{F-F}$ = 59 Hz), −97.9 (dq, 1F, C=CF_{trans} $^4J_{F-F}$ = 24 Hz, $^2J_{F-F}$ = 59 Hz).

2-Ketopentafluoropropanesulfonic Acid (*3*). Dropwise addition of sulfur trioxide (20.8 mL, 0.499 mol) to a flask containing neat **1** (92.0 g, 0.522 mol) chilled to 0 °C produced an exothermic reaction within minutes, resulting in a dark brown solution. The ice bath was removed, and the mixture was stirred for 2 h at room temperature to ensure completion. Trifluoroacetic acid (60 g, 0.53 mol) was added to convert any sulfonic ester, **2**, to the sulfonic acid, **3**, and the reaction mixture was stirred overnight at 50 °C. Vacuum distillation of the mixture resulted in isolation of a tinted, fuming liquid, 2-ketopentafluoropropanesulfonic acid (**3**) (61 g, 51%, bp = 95−100 °C at 2−3 mmHg). **3** was stored in a sealed round-bottom flask at 0 °C.

Scheme 2. Synthesis of *N,N*-Diisopropylethylammonium 2,2-Bis(*p*-hydroxyphenyl)pentafluoropropanesulfonate (HPPS) (4)

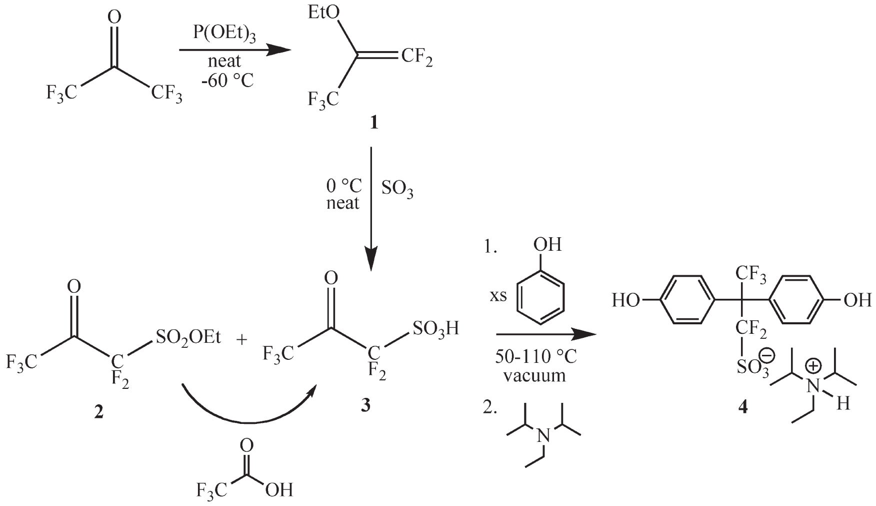

N,N-Diisopropylethylammonium 2,2-Bis(p-hydroxyphenyl)pentafluoropropanesulfonate (***4***). To a flask containing neat **3** (48.1 g, 0.211 mol) was added excess (43.0 g, ~2.2 mol) phenol. An exothermic reaction occurred immediately, resulting in a viscous orange solution. The mixture was initially stirred under vacuum at 50 °C, and the temperature was gradually raised to 110 °C over the course of 3 h. During this time the reaction mixture solidified and became dark brown. The acidic product was neutralized with a solution of *N,N*-diisopropylethylamine (30 g) and water (200 mL) and stirred at 75 °C for 1 h. The water layer was decanted, leaving an amber-colored oil that was dissolved in acetone at 50 °C. The solution was allowed to cool to room temperature, and slow addition of diethyl ether formed a flaky yellow precipitate. The acetone/ether layer was decanted to remove organic byproduct. THF was poured into the flask to wash away additional organic products, and a pale yellow solid was collected by filtration and dried in vacuo (67.1 g, 60%, mp = 189.3 °C). IR (PTFE film): ν_{O-H} = 3301 cm^{-1}. ^{1}H NMR (DMSO-d_6, 298 K, δ): 9.50 (s, 2H, OH), 8.13 (br s, 1H, NH), 7.26 (d, 4H, Ar), 6.66 (d, 4H, Ar), 3.57 (m, 2H, Me$_2$CHN), 3.09 (q, 2H, CH_2N), 1.21 (t, 12H, CH(CH_3)$_2$), 1.21 (t, 3H, CH$_2$CH_3). ^{13}C NMR (CD$_3$OD, 298 K, δ): 13.3 (CH$_2$CH$_3$), 30.8 (CH$_2$CH$_3$), 43.9 (CHMe$_2$), 55.8 (CH(CH$_3$)$_2$), 66.2 (m, CF$_3$CCF$_2$), 114.7, 126.8, 134.2, 158.3 (Ar), 123.05 (t, CF$_2$, $^1J_{C-F}$ = 293 Hz), 126.9 (q, CF$_3$, $^1J_{C-F}$ = 287 Hz). ^{19}F NMR (CD$_3$OD, 298 K, δ): −62.1 (t, 3F, CF_3), −92.8 (q, 2F, CF_2). Analysis for $C_{23}H_{30}F_5NO_5S$ (wt %): Calculated: C, 52.35; H, 5.74; N, 2.66. Found: C, 52.09; H, 5.61; N, 2.83.

Homopolymerization of HPPS (4) and FPS. To a 250 mL three-neck, round-bottom flask equipped with mechanical stirrer, nitrogen purging adapter, and reflux condenser were charged **4** (98.7%) (1.0133 g, 1.8957 mmol), bis(4-fluorophenyl) sulfone (FPS) (0.4944 1.9447 mmol), DMAc (6.0 mL), and K$_2$CO$_3$ (0.55 g, 3.99 mmol). With mechanical stirring and under slow nitrogen purge, the reaction was heated at 180 °C overnight using an oil bath. The reaction was cooled down to room temperature, and 2.0 mL of DMAc was added to the flask to replace that which was lost due to evaporation and to adjust the viscosity for precipitation. Water (200 mL) was added to the flask to precipitate the product. The polymer remained in water overnight and then was dried under vacuum, yielding 1.04 g of product.

Copolymerization of HPPS (4), BP, and FPS. A procedure similar to that used for the homopolymer was used for the copolymer synthesis. The amounts of the starting materials and the products are shown in Table 1. The copolymers were named as PEAS-20, PEAS-31, PEAS-40, PEAS-49, and PEAS-61, where the numerical suffix denotes the mole percentage of sulfonated polymer repeating units, i.e., $m \times 100\%/(m + n)$ in Scheme 1.

Performance Properties Measurements. *Film Casting and Membrane Acidification.* The copolymers, in K-salt form, were dissolved in DMAc to obtain solutions with a concentration of 5% w/v. The solutions were filtered through 0.45 μm Teflon syringe filters and cast onto clean Teflon dishes. The films were dried for 12 h in a vacuum oven with air circulation at 60 °C. Residual solvent was removed by further drying the films under vacuum for 24 h at 120 °C. The fully dried films were removed from the Teflon dishes, and the free-standing membranes were converted to the acid form by boiling in 0.5 M sulfuric acid for 2 h, followed by boiling in DI water for 2 h. The membranes were removed from the water and stored within a humidity chamber (30% RH, 25 °C) until further use. The membranes thus obtained were ~50 μm thick, mechanically robust, and easily handled.

Determination of Ion Exchange Capacity (*IEC*). The acidified membranes were dried under vacuum at 120 °C for 24 h. Each membrane was weighed and then stirred in an excess, known volume of 0.1 M NaOH for 12 h to ensure that the membrane was completely neutralized. Excess NaOH was then titrated using 0.01 M acetic acid and a phenylphthalein indicator. IEC was then calculated based on the weight of the acidified membrane and the moles of NaOH consumed during neutralization of the membrane, determined by difference.

Determination of Water Uptake. Equlibrium water uptake of the copolymers, at 80 °C over a range of relative humidity (RH), was measured by subjecting the hydrated samples to an isothermal desorption using a TA Q5000SA moisture analyzer. The samples were examined over the range of 10−90% RH by decreasing the humidity 10% per hour. The hydration number (λ), which is defined as the number of water molecules per sulfonic acid group, was calculated using IEC values obtained from titration of the acidified membranes and the following equation

$$\lambda = \frac{(W_{\rm wet} - W_{\rm dry})/{\rm MW}_{\rm H_2O}}{{\rm IEC} \times W_{\rm dry}} \times 1000$$

where $W_{\rm dry}$ is the weight of the sample at 0% RH, $W_{\rm wet}$ is the weight of the sample at a particular humidity, and ${\rm MW}_{\rm H_2O}$ is the molecular weight of water (18.01 g/mol).

Determination of Proton Conductivity. Proton conductivities of the acidified membranes were measured at 80 °C using a BekkTech conductivity analyzer. The samples were examined over the range of 20−100% RH with a 10% RH increase per hour.

Results and Discussion

Synthesis of Ion-Containing Bisphenolic Monomer, HPPS (4). Scheme 2 shows the three-step synthesis of **4**. This procedure

Table 1. Comonomer Charge Amounts and Copolymer Yield for Copolymerizations

	FPS		HPPS (4)		BP		
copolymer	(g)	(mmol)	(g)	(mmol)	(g)	(mmol)	copolymer yield (g)
PEAS-20	0.7943	3.1240	0.3205[a]	0.6008	0.4563[b]	2.4675	1.23
PEAS-31	0.7873	3.0965	0.4818[a]	0.9031	0.3976[b]	2.1501	1.32
PEAS-40	0.7777	3.0588	0.6401[c]	1.2060	0.3380[d]	1.8006	1.47
PEAS-49	0.7775	3.0580	0.8003[c]	1.5078	0.2817[d]	1.5007	1.53
PEAS-61	0.7797	3.0666	0.9647[c]	1.8176	0.2257[d]	1.2023	1.59

[a] Purity of monomers back-calculated from polymerization degree: 98.9%. [b] 100.7%. [c] 99.4%. [d] 99.2%.

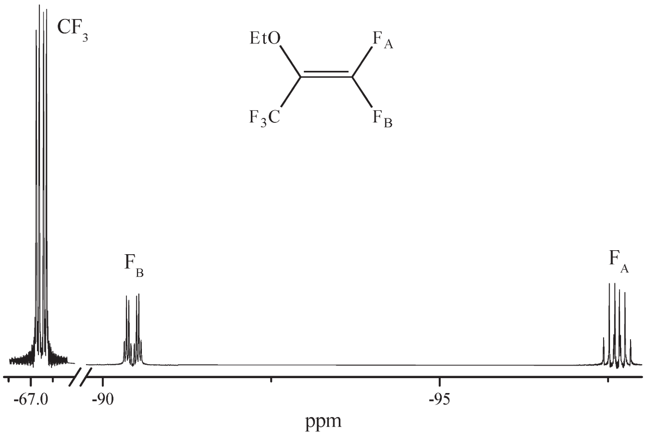

Figure 1. Expanded ^{19}F NMR spectrum of **1**.

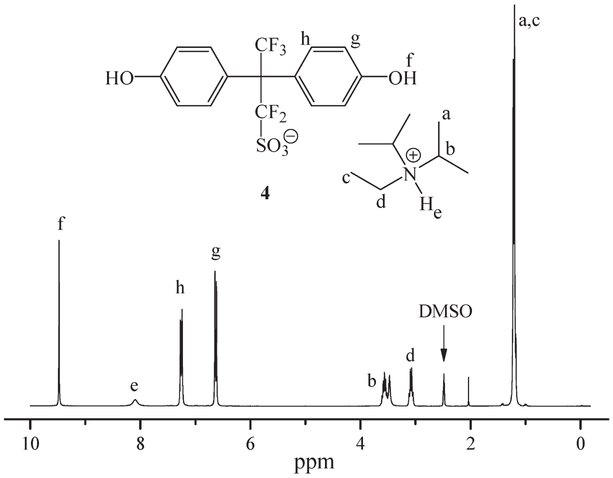

Figure 2. ^{1}H NMR spectrum of HPPS (**4**).

exploits the highly electrophilic nature of ketones with adjacent perfluoroalkyl units:[18,19] once in formation of the vinyl ether intermediate, **1**, and again during the condensation reaction of phenol and **3**. All three reactions of Scheme 2 proceeded quickly, and sometimes violently, especially in forming **1**.

In step one, we improved upon an earlier synthesis of ethyl pentafluoroisopropenyl ether, **1**.[20] Slow addition of triethyl phosphite into neat hexafluoroacetone at −60 °C under nitrogen afforded the clear, colorless isopropenyl ether after distillation in yields of 75−80%, increased from 50% as reported earlier.

The ^{1}H NMR spectrum of **1** depicts the ethoxy group only and is unremarkable. ^{13}C and ^{19}F NMR spectra were more complex due to the influence of fluorine. The ^{13}C NMR spectrum (Figure A, Supporting Information) features the CF_3 carbon (Figure A1) as a doublet of doublet of quartets centered at 120.9 ppm with three unique coupling values. Each of the two vinylic fluorine atoms exerts a separate three-bond coupling constant on the trifluoromethyl carbon due to hindered rotation about the double bond. The $=CF_2$ carbon (Figure A2) appears as a pseudo-triplet of multiplets, although the triplet is not in a true 1:2:1 ratio due to the inequivalency of the vinylic fluorine atoms. The poorly resolved internal olefinic carbon resonates as a complex multiplet centered around 112 ppm. The ^{19}F NMR spectrum (Figure 1) clearly shows three resonances. The trifluoromethyl moiety appears as a doublet of doublets, again reflecting the unique cis (10 Hz) and trans (24 Hz) coupling to the vinylic fluorine atoms. It should be noted that four-bond coupling is common for larger atoms like fluorine, since coupling arises from s-orbital overlap. Each vinylic fluorine atom resonance resolves as a doublet of quartets with evident geminal coupling (59 Hz) and respective cis/trans coupling.

Sulfonation of **1** with sulfur trioxide yielded a mixture of the sulfonate ester, **2**, and the desired sulfonic acid, **3**.[21,22] This reaction proceeds through a sultone intermediate that decomposes at room temperature to a mixture of β-ketosulfonate ester and β-ketosulfonic acid.[22] Because of the lack of electron density in the double bond, sulfur trioxide must be used rather than milder sulfonation agents. The product mixture was treated with trifluoroacetic acid to convert the sulfonate ester to **3**. Excess acid and resultant ethanol were easily removed via vacuum distillation at 50 °C, prior to vacuum distillation of **3** around 95 °C.

Condensation of **3** with 2 equiv of phenol and subsequent neutralization with *N*,*N*-diisopropylethylamine afforded *N*,*N*-diisopropylethylammonium 2,2-bis(*p*-hydroxyphenyl)-pentafluoropropanesulfonate, **4**, in fair yields (≈60%).[21] Krespan previously reported the synthesis of the pyridinium salt of **4**,[21] and a recent patent application disclosed polymers synthesized using the potassium salt of **4**, although no experimental data were given.[23] After experimentation with several alternative neutralizing agents including pyridine and alkali metal hydroxides and carbonates, we determined that the aliphatic tertiary amine, *N*,*N*-diisopropylethylamine, produces a salt with favorable solubility and crystallization behavior. It is sparingly soluble in water, which facilitates isolation, and as will be shown, it may be used directly in polymerization, and under these conditions, the free amine is released and volatilized out of the polymer product.

The ^{1}H NMR spectrum of **4** (Figure 2) features a two doublet pattern (6.66 and 7.26 ppm) in the aromatic region characteristic of para substitution on the phenol ring. Several peaks attributed to the ammonium counterion appear upfield (3.57, 3.09, 1.21, and 1.21 ppm). Using DMSO as solvent, the hydroxy protons resonate sharply at 9.50 ppm, and the ammonium proton appears as a broad singlet at 8.13 ppm. Integration indicates the presence of two aromatic rings in the product due to the 4:2 ratio of each aromatic peak to the isopropyl protons (3.57 ppm) in the counterion. Fluorine NMR

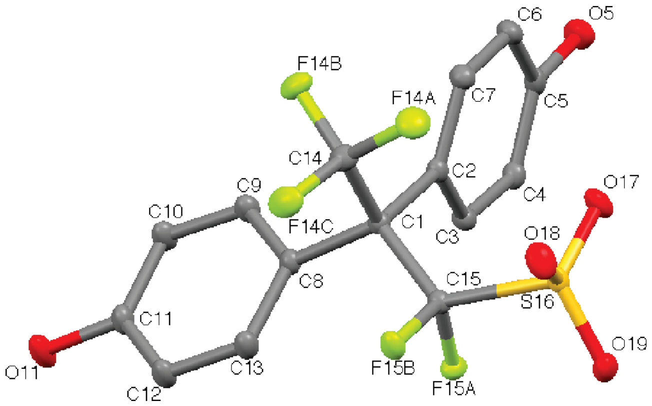

Figure 3. Thermal ellipsoid diagram of *N*,*N*-diisopropylethylammonium 2,2-bis(*p*-hydroxyphenyl)pentafluoropropanesulfonate, HPPS (**4**). Hydrogen atoms and counterions are omitted for clarity.

Scheme 3. Synthesis of Homopoly(arylene ether sulfone) Synthesized from HPPS (4) and FPS

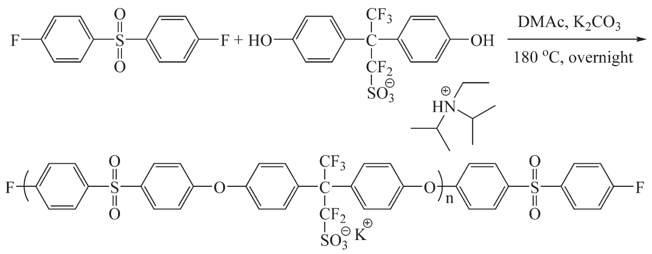

data yield the expected triplet (CF_3) and quartet (CF_2) at −62.1 and −92.8 ppm, respectively.

Single crystals of **4** suitable for X-ray diffraction were grown via evaporation from a concentrated methanol solution. Pale brown blocks formed after several days. The crystal structure thus obtained (Figure 3) confirmed assignment of **4** as a 4,4′-bisphenolic molecule with a pendant perfluorinated sulfonate unit. The newly formed quaternary carbon, C1, serves as the junction between the two phenol rings and the perfluoroalkyl sulfonate tether and adopts a tetrahedral geometry. Delocalization of the negative charge in the sulfonate unit is evident: all S−O bonds are ~1.45 Å.

Homopolymerization of HPPS (4) and FPS. Step-growth polymerization of **4** and FPS via nucleophilic aromatic substitution was performed in DMAc at 180 °C in the presence of K_2CO_3 (Scheme 3). Condensation products of the reaction consisted of CO_2, KF, and water. Also, under these conditions the diisopropylethylammonium cations associated with the ionic comonomer were decomposed and replaced by potassium, with concomitant release of the free amine. Traditionally for poly(arylene ether sulfone) preparations, toluene has been used as an azeotroping agent to drive the reaction to completion. However, codistillation of the toluene-miscible diisopropylethylamine was found to prevent efficient separation of water in the Dean−Stark receiving flask. We therefore discontinued the use of toluene and instead used a slow N_2 purge to sweep water and diisopropylethylamine from the reactor headspace. After cooling, the polymer was precipitated by addition of water. High molecular weight product was obtained as indicated by NMR and GPC analysis, and the procedure was deemed effective.

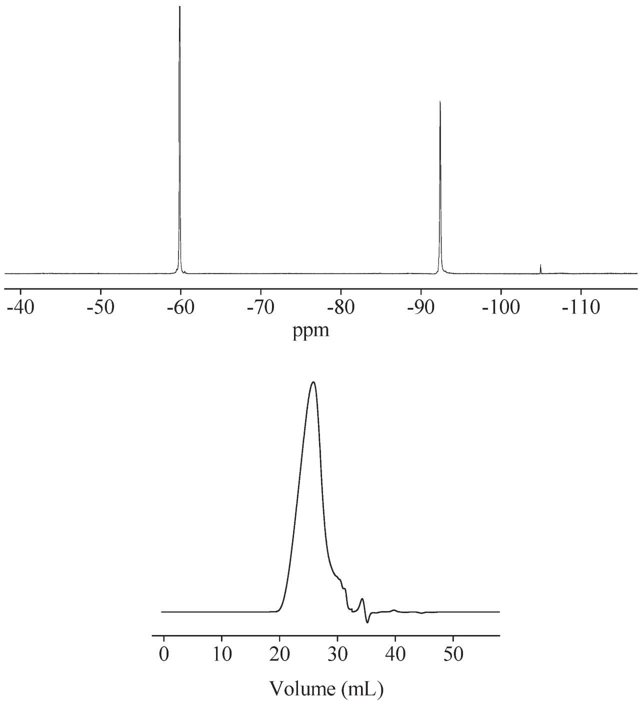

Figure 4. ^{19}F NMR spectrum and GPC trace for homopoly(arylene ether sulfone) synthesized from **4** and FPS. Top: ^{19}F NMR spectrum. Ratio of peak integration is 59.68:39.29:1.03; M_n was calculated to be 25 100 g/mol. Bottom: GPC trace (RI signal). M_n was determined to be 19 300 g/mol.

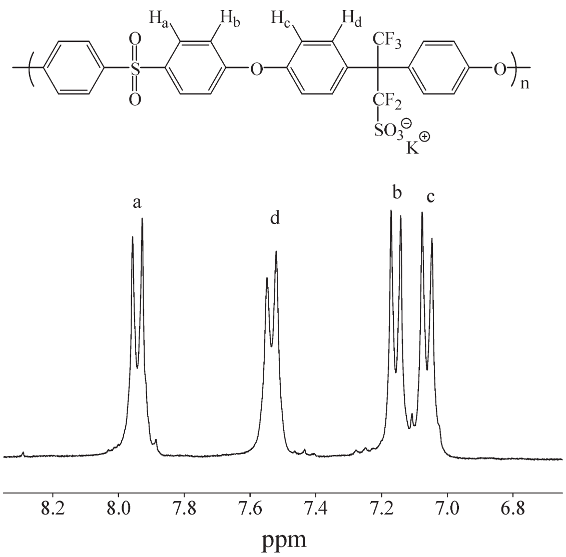

Figure 5. Expanded ^{1}H NMR spectrum of homopoly(arylene ether sulfone) synthesized from HPPS (**4**) and FPS.

The homopolymerization was formulated using a slight stoichiometric excess of FPS; thus, the resulting polymer possessed fluorophenyl end groups, and control of molecular weight was achieved by adjusting the excess molar ratio of FPS. In the ^{19}F NMR spectrum of the product (Figure 4, top), three peaks were found at −60 (triplet, $-CF_3$), −93 (doublet, $-CF_2-$), and −105 ($-F$, singlet). The first two were assigned to the structural units of HPPS within the polymer, whereas the latter represents the terminal fluorophenyl moieties. Assuming the polymer structure shown in Scheme 3, the intensity ratio of the $-CF_2-$ and $-F$ peaks provides a measure of the polymerization degree of the polymer. This value was determined to be 38.15, and correspondingly, the M_n of this polymer was calculated to be 25 100 g/mol. According to GPC data (Figure 4, bottom), the M_n and M_w were determined to be 19 300 and 33 600 g/mol, respectively.

Table 2. Composition and Molecular Weights of Copolymers from HPPS (4), BP, and FPS

copolymer	composition (theo)[a]	composition (NMR)[b]	$M_{n,theo}$ (g/mol)	$M_{n,NMR}$ (g/mol)	$M_{n,GPC}$ (g/mol)	M_w/M_n
PAES-20	20/80	20/80	25 000	27 100	28 400	1.63
PAES-31	30/70	31/69	33 700	31 900	27 500	1.76
PAES-40	40/60	40/60	29 100	27 800	38 700	1.63
PAES-49	50/50	49/51	32 200	31 400	33 700	1.88
PAES-61	60/40	61/39	35 900	28 500	29 900	2.11

[a] From comonomer feed ratios in Table 1. [b] m/n, Figure 6, determined by ^{1}H NMR.

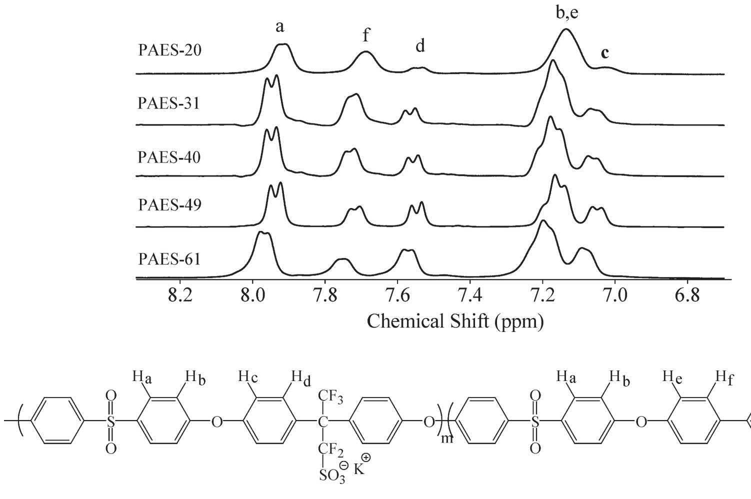

Figure 6. ^{1}H NMR spectra and assignments of copolymers from HPPS (4), BP, and FPS.

The ^{1}H NMR spectrum of the homopolymer is shown in Figure 5. The entire spectrum consisted of four doublets of equal intensity within the aromatic region. Because of the symmetry and simplicity of the polymer repeating unit, each peak was easily assigned, as indicated. No peaks for the diisopropylethylammonium were found in the spectrum, confirming that the associated cations were exclusively potassium.

In a polycondensation reaction, precise control of comonomer stoichiometry is crucial to achieve high molecular weight. Therefore, one must have an accurate measure of the effective equivalent weight of each monomer, which is determined by monomer purity. Commercially available FPS was further purified by recrystallization in toluene and was assumed to be essentially 100% pure. **4** was purified by recrystallization in acetonitrile. The purity of **4** was estimated by polymerizing it with a slight excess of FPS and then back-calculating its purity from the polymerization degree, which was easily obtained from the ^{19}F NMR spectrum. In this way, the purity of recrystallized **4** was calculated to be 98.7%.

Copolymerization of HPPS (4), BP, and FPS. Fuel cell membrane materials should have an appropriate balance of hydrophobic character for membrane stability and strength and hydrophilic character for water swelling and proton conduction. Increased hydrophobic character was introduced by employment of biphenol (BP) as a comonomer. Using a procedure similar to that used for the homopolymer, five copolymers with varying amounts of hydrophobic and hydrophilic repeating units were synthesized from BP, **4**, and FPS (Table 2). Excess FPS was used for molecular weight control. BP was purified by vacuum sublimation, and its purity was estimated using trial polymerization with FPS, followed by ^{19}F NMR analysis, in the same way as for **4**.

^{1}H NMR was used to determine composition of the copolymers (Figure 6). All peaks were contained within the aromatic region from 8.1 to 6.9 ppm. Peaks b, c, and e located farthest upfield were assigned to the protons positioned ortho to an electron-donating ether oxygen, in both copolymer repeat units. For purposes of calculating copolymer composition, the farthest downfield peak a, representing the four protons ortho to the electron-withdrawing sulfone group, was used as an internal reference since its intensity does not change with copolymer composition. Peaks f and d, which appear in the middle of the range and are well separated, were assigned to the inner aromatic protons of the BP and **4** structural units, respectively, and were used to characterize their molar ratio in the copolymer. The copolymer composition data thus obtained, expressed as m/n (see Figure 6), are listed in Table 2.

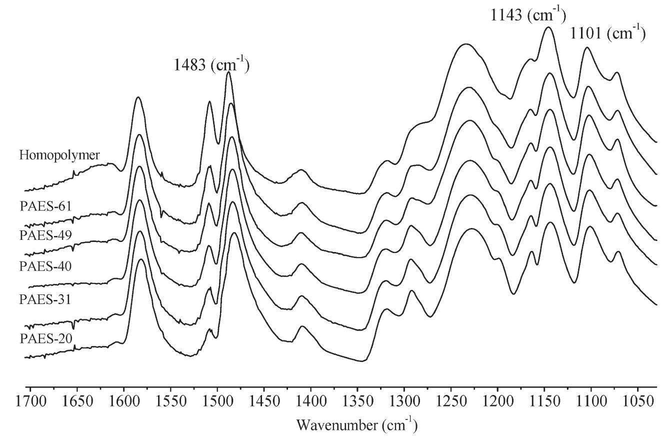

Figure 7. ATR-FTIR spectra of PAES homo- and copolymers.

The copolymers were also analyzed using ^{19}F NMR and GPC. In general, all copolymers were difficultly soluble and could be dissolved only in dipolar aprotic solvents including DMF, DMAc, and DMSO. GPC of the copolymers was performed using a mobile phase consisting of DMF containing 0.02 M LiBr on account of the presence of the ionic sulfonate units. Multiangle laser light scattering provided

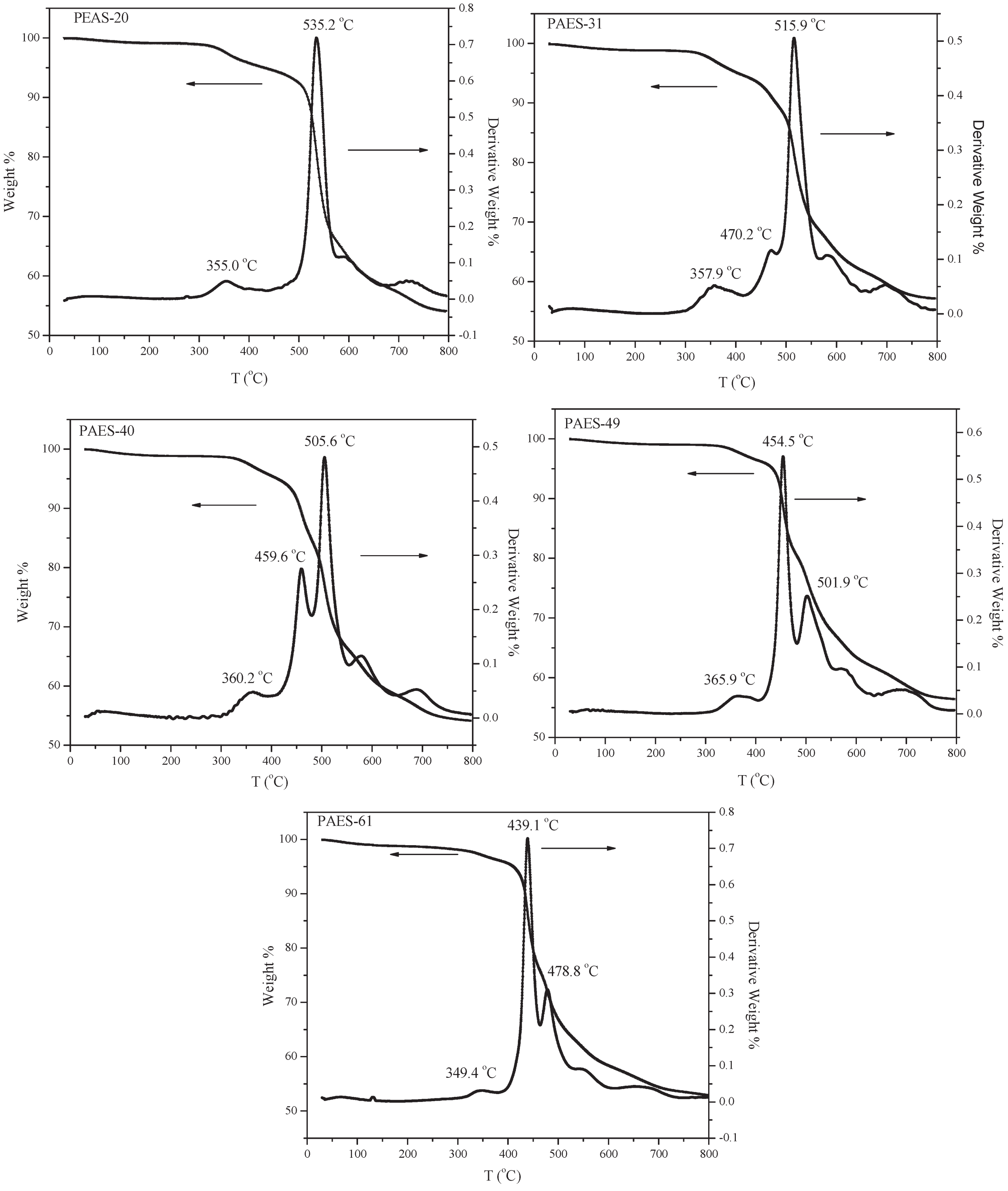

Figure 8. TGA traces of PAES copolymers (potassium salt form) under nitrogen (10 °C/min).

absolute molecular weights; dn/dc values were calculated using the 100% mass recovery assumption. Theoretical M_n was defined by the ratio of fluorophenyl to phenolic functionality; the gram amounts, and molar amounts corrected for purity, of all monomers can be found in Table 1. As Table 2 shows, good agreement was obtained between M_n's detected by GPC and ^{19}F NMR. M_n of the copolymer series varied from 27 900 to 32 600 (by ^{19}F NMR). It should also be noted that on the basis of purity estimation of each monomer it was possible to obtain copolymers with roughly similar M_n using three monomers of different purity.

ATR-FTIR was performed directly on samples of the copolymers and homopolymer (K-salt form) obtained by precipitation of the polymerization reaction into water and subsequent vacuum drying (Figure 7). In the fingerprint area of each spectrum, a strong band was found at 1240 cm^{-1}, representing the C$-$O stretch of the ether linkage. Vibrations of sulfonic acid groups in sulfonated poly(arylene ether sulfone) have been reported at 1026 (symmetric stretching) and 1082 cm^{-1} (asymmetric stretching)[24] or 1030 (symmetric stretching) and 1112 cm^{-1} (asymmetric stretching).[25] We found analogous vibrations at 1101 and 1143 cm^{-1}. However,

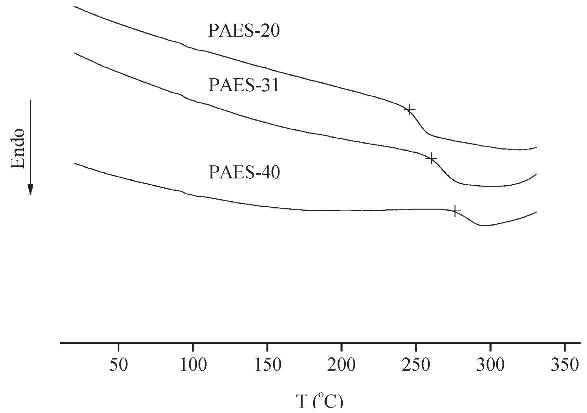

Figure 9. DSC traces for PEAS-20, PEAS-31, and PEAS-40.

Table 3. IECs and Conductivity Data of PAES Copolymers

	IEC_{NMR} (mequiv/g)	IEC_{TITR} (mequiv/g)	conductivity[a] (mS/cm)
PAES-20	0.44	0.36	1.6
PAES-31	0.65	0.63	1.4
PAES-40	0.80	0.84	2.5
PAES-49	0.94	1.08	21
PAES-61	1.10	1.25	23

[a] 80 °C, 100% RH.

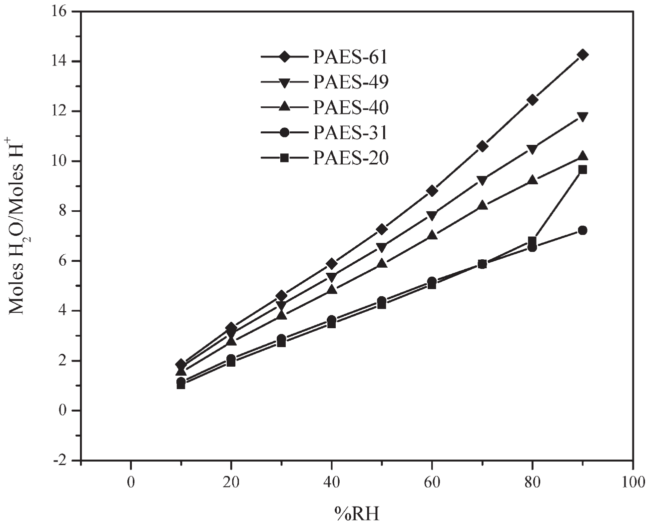

Figure 10. Water uptake vs relative humidity of PAES copolymers.

since these vibrations were observed to overlap with those due to sulfone symmetric stretching, it was difficult to correlate their intensity with differences in the concentration of sulfonic acid repeating units in the various copolymers. Because of several aromatic rings within the copolymers, strong peaks were found in the region from 1475 to 1600 cm^{-1}. The peak at 1515 cm^{-1} was assigned to the C=C ring stretches for the 2,2-diphenylperfluorinated propanesulfonic acid moieties. The peaks at 1588 and 1490 cm^{-1} were assigned to C=C ring stretching absorptions of the phenyl sulfone moiety. These two peaks were red-shifted since the phenyl ring is conjugated with the electron-withdrawing sulfone group. Contributions from the bisphenoxy group in this region were difficult to identify. Medium-intensity peaks were observed at 1612, 1589, and 1492 cm^{-1} in the spectrum of free biphenol monomer, but analogous peaks could not be definitively assigned in the copolymers. Presumably the latter two peaks were merged into strong peaks observed at 1588 and 1490 cm^{-1} in the spectra of copolymers. The intensity ratio of peaks at 1515 and 1490 cm^{-1} reflected the molar ratio of 2,2-diphenylperfluorinated propanesulfonic acid to biphenyl sulfone moieties. These results were consistent with the NMR data.

TGA was used to determine thermal stability of the PAES copolymers (K-salt form) produced from HPPS, BP, and FPS. Figure 8 shows the various traces obtained. Analyses were run under nitrogen at a temperature ramp of 10 °C/min. In each spectrum, both cumulative and instantaneous (first derivative) weight loss are shown. Although all copolymers were annealed at 120 °C under vacuum overnight, minor weight losses were still observed between 20 and 200 °C due to release of residual moisture. As indicated by the first-derivative weight loss curves, all five copolymers showed multistep decomposition patterns, with an initial, minor loss process centered in the range 350−365 °C. For PAES-20, the copolymer containing the lowest fraction of ionic comonomer, this initial loss (~6 wt %) was close to the theoretical weight percentage of $-SO_3K$ groups in the entire polymer (5.28 wt %), suggesting that decomposition begins by cleavage of the sulfonate moiety. This is consistent with the observations of McGrath et al., who reported two distinct decomposition steps for sPAES: an earlier (lower temperature) cleavage of side sulfonic acid groups and a later (higher temperature) breakup of the polymer main chain;[14] even though in the latter polymers the sulfonate group is attached to an aromatic ring, whereas in the present polymers it is attached to an aliphatic perfluoro side chain. A second loss process, visible at 470.2 °C in the first-derivative curve for PAES-31, became increasingly dominant with increasing ionic comonomer content and was the most important decomposition process for PAES-49 and PAES-61. The peak temperature of this process steadily decreased from 470.2 to 439.1 °C with increasing ionic content, indicating that in general thermal stability decreases as the fraction of ionic repeating units increases. The theoretical weight percentage of $-SO_3K$ groups exceeds the mass loss of the first degradation step for all four copolymers with higher ionic contents. If the first degradation process indeed represents sulfonate group cleavage, then the second degradation process must involve both sulfonate cleavage and main-chain decomposition. This process may be similar to the thermolysis of Nafion, in which side-group cleavage and main-chain breakup have been observed to occur simultaneously, resulting in one broad decomposition process.[26−28]

In DSC analysis of the PAES copolymers, the specimen was heated at a rate of 10 °C/min from −20 to 300 °C and held for 5 min to eliminate any thermal history of the sample. The temperature was then quenched back to −20 °C, and the spectrum was recorded in the second heating cycle with the same heating rate. DSC was performed on all samples; however, since the T_g of the copolymers is very close to the degradation temperature, only PAES-20, PAES-31, and PAES-40 gave useful spectra (Figure 9). An obvious glass transition was found at 242, 260, and 273 °C (onset) for PAES-20, PAES-31, and PAES-40, respectively. The data show that introduction of the perfluorinated propanesulfonate (K salt) moiety reduces the thermal motion of the polymer chains and increases the glass transition temperature. In general, the relatively high T_g's of these materials are favorable and suggest a potentially wide range of working temperatures in a fuel cell.

Ion Exchange Capacity, Water Uptake, and Proton Conductivity of Copolymers from BP, HPPS, and FPS. Varying the BP/HPPS comonomer ratio allowed a determination of the effect of IEC on water uptake and conductivity of the copolymers. IEC values were calculated using the monomer ratios obtained from ^{1}H NMR, shown in Table 2, and the molecular weight of the repeat units. After film casting and membrane acidification, the IEC was determined by titration to confirm the effectiveness of the membrane acidification procedure. Table 3 shows the IEC values from both NMR and titration measurements as well as the conductivity of the membranes at 80 °C and 100% RH. Water uptake, expressed as the hydration number (λ = mol H_2O/mol sulfonic acid), was plotted versus % RH in Figure 10.

The new copolymers exhibited the expected trend of increasing water uptake and conductivity with increasing IEC. The water uptake values at 90% RH (Figure 10) agree closely with published water uptake data for sPAES membranes of similar composition and IEC, but having ionic structural units derived from 3,3′-disulfonate-4,4′-dichlorodiphenyl sulfone, under fully hydrated conditions.[13] However, the conductivity values achieved by the new copolymers were much lower than expected. This is likely due to a relatively low fraction of sulfonate groups involved in large, interconnected hydration shells, which would aid proton transport. Incorporation of HPPS comonomer, with only a single perfluoroalkyl sulfonate group, apparently leads to a high fraction of isolated acid groups, which are able to absorb water molecules but are unable to form an interconnected hydration shell with other acid groups and hence do not contribute substantially to conductivity.

Summary and Conclusion

The fluorosulfonate monomer, *N,N*-diisopropylethylammonium 2,2-bis(*p*-hydroxyphenyl)pentafluoropropanesulfonate, **4**, was synthesized via condensation of phenol with 2-ketopentafluoropropanesulfonic acid, followed by neutralization with *N,N*-diisopropylethylamine. The acid was prepared by reaction of ethyl pentafluoroisopropenyl ether with liquid sulfur trioxide. Homopolymerization of **4** with FPS was performed, and a procedure was developed to yield high molecular weight product. Using varying molar ratios of **4** and BP, a series of copolymers was prepared with FPS. Purity estimation of each monomer was achieved via back-calculation from observed molecular weight of trial copolymers. By employing slight excess amounts of FPS, molecular weights were controlled. Chemical structures of the homo- and copolymers were determined using ^{1}H NMR and FTIR spectroscopy, and molecular weights were characterized using ^{19}F NMR spectroscopy and GPC. Close agreement between theoretical and experimental M_ns of the copolymers confirmed the reliability of the methods. Thermal analysis of the copolymers revealed that T_gs were in the range 240−275 °C and increased with increasing ionic content (DSC) and thermal stability generally decreased with increasing ionic content (TGA).

Free-standing films of the copolymers in the acid form were subjected to ion exchange capacity, water uptake, and conductivity measurements. Ion exchange capacity determined by titration agreed well with theoretical values determined by NMR characterization. HPPS-containing copolymers had similar water-uptake values but lower proton conductivities compared to 3,3′-disulfonate-4,4′-dichlorodiphenylsulfone-containing copolymers. It was hypothesized that incorporation of HPPS comonomer, with only a single perfluoroalkyl sulfonate group, leads to a high fraction of isolated acid groups, which attract water molecules but are unable to form an interconnected hydration shell with other acid groups and hence do not contribute substantially to conductivity. Possible approaches toward improving the performance of HPPS-based PAES include creation of multiblock copolymers consisting of HPPS-rich hydrophilic blocks and PAES hydrophobic blocks,[16,17] modification of HPPS to place the sulfonic acid group at the end of a longer perfluoroalkylene tether and thus away from the backbone, addition of flexible groups along the backbone to promote molecular mobility and aggregation of the ion exchange moieties, and incorporation of HPPS as a supplemental ionic comonomer within sPAES.

Acknowledgment. The authors gratefully acknowledge financial support provided by the Department of Energy, grant DE-FG36-086O88106, and Dr. Jeffrey R. Deschamps, Naval Research Laboratory, for determination of the X-ray crystal structure of HPPS.

Supporting Information Available: Expanded ^{13}C NMR spectra of **1** showing the $-CF_3$ and $=CF_2$ resonances. This material is available free of charge via the Internet at http://pubs.acs.org.

References and Notes

(1) O'Hayre, R. P.; Cha, S.-W.; Colella, W.; Prinz, F. B. *Fuel Cell Fundamentals*; John Wiley & Sons: New York, 2009.

(2) Hickner, M. A.; Ghassemi, H.; Kim, Y. S.; Einsla, B. R.; McGrath, J. E. *Chem. Rev.* **2004**, *104*, 4587–4612.

(3) Viswanathan, B.; Helen, M. *Bull. Catal. Soc. India* **2007**, *6*, 50–66.

(4) Decker, B.; Hartmann-Thompson, C.; Carver, P. I.; Keinath, S.; Santurri, P. *Chem. Mater.* **2010**, *22*, 942–948.

(5) Jalani, N. H.; Dunn, K.; Datta, R. *Electrochim. Acta* **2005**, *51*, 553–560.

(6) Deng, Q.; Moore, R. B.; Mauritz, K. A. *J. Appl. Polym. Sci.* **1998**, *68* (5), 747–763.

(7) Cho, E.-B.; Kim, H.; Kim, D. *J. Phys. Chem. B* **2009**, *113* (29), 9770–9778.

(8) Horan, J. L.; Genupur, A.; Ren, H.; Sikora, B. J.; Kuo, M.-C.; Meng, F.; Dec, S. F.; Haugen, G. M.; Yandrasits, M. A.; Hamrock, S. J.; Frey, M. H.; Herring, A. M. *ChemSusChem* **2009**, *2* (3), 226–229.

(9) Yameen, B.; Kaltbeitzel, A.; Langer, A.; Müller, F.; Gösele, U.; Knoll, W.; Azzaroni, O. *Angew. Chem., Int. Ed.* **2009**, *48* (17), 3124–3128.

(10) Kwon, Y. H.; Kim, S. C.; Lee, S.-Y. *Macromolecules* **2009**, *42* (14), 5244–5250.

(11) Li., Y.; Wang, F.; Yang, J.; Liu, D.; Roy, A.; Case, S.; Lesko, J.; McGrath, J. E. *Polymer* **2006**, *47* (11), 4210–4217.

(12) Chhabra, P.; Choudhary, V. *Eur. Polym. J.* **2009**, *45* (5), 1467–1475.

(13) Wang, F.; Hickner, M.; Kim, Y. S.; Zawodzinski, T. A.; McGrath, J. E. *J. Membr. Sci.* **2002**, *197*, 231–242.

(14) Kim, Y. S.; Dong, L.; Hickner, M. A.; Pivovar, B. S.; McGrath, J. E. *Polymer* **2003**, *44*, 5729–5736.

(15) Wiles, K. B.; Wang, F.; McGrath, J. E. *J. Polym. Sci., Part A: Polym. Chem.* **2005**, *43* (14), 2964–2976.

(16) Ghassemi, H.; McGrath, J. E.; Zawodzinski, T. A., Jr. *Polymer* **2006**, *47*, 4132–4139.

(17) Lee, M.; Park, J. K.; Lee, H.-S.; Lane, O.; Moore, R. B.; McGrath, J. E.; Baird, D. G. *Polymer* **2009**, *50*, 6129–6138.

(18) Rogers, F. E.; Rapiejko, R. J. *J. Am. Chem. Soc.* **1971**, *93* (18), 4596–4597.

(19) Lindner, P. E.; Lemal, D. M. *Tetrahedron Lett.* **1996**, *37* (51), 9165–9168.

(20) Wiley, D. W.; Simmons, H. E. *J. Org. Chem.* **1964**, *29* (7), 1876–1879.

(21) Krespan, C. G. *J. Org. Chem.* **1979**, *44* (26), 4924–4929.

(22) Krespan, C. G.; Smart, B. E.; Howard, E. G. *J. Am. Chem. Soc.* **1977**, *99* (4), 1214–1217.

(23) Koolpe, G.; Ventura, S. C. U.S. Patent Application Publication 2007/0065700, March 22, 2007.

(24) Pan, H.; Zhu, X.; Chen, J.; Jian, X. *J. Membr. Sci.* **2009**, *326* (2), 453–459.

(25) Lee, J. K.; Li, W.; Manthiram, A. *J. Membr. Sci.* **2009**, *330*, 73–79.

(26) Wilkie, C. A.; Thomsen, J. R.; Mittleman, M. L. *J. Appl. Polym. Sci.* **1991**, *42* (4), 901–909.

(27) Deng, Q.; Wilkie, C. A.; Moore, R. B.; Mauritz, K. A. *Polymer* **1998**, *39* (24), 5961–5972.

(28) Chen, C.; Fuller, T. F. *Polym. Degrad. Stab.* **2009**, *94* (9), 1436–1447.